www.czasopisma.pan.pl PAN www.journals.pan.pl

Metrol. Meas. Syst., Vol. 24 (2017), No. 4, pp. 645–652.

METROLOGY AND MEASUREMENT SYSTEMS

Index 330930, ISSN 0860-8229

www.metrology.pg.gda.pl

MEASUREMENT OF NOISE IN SUPERCAPACITORS

Arkadiusz Szewczyk

Gdańsk University of Technology, Faculty of Electronics, Telecommunications and Informatics, G. Narutowicza 11/12, 80-233 Gdańsk, Poland (✉ szewczyk@eti.pg.edu.pl, +48 58 347 2140)

Abstract

A developed method and measurement setup for measurement of noise generated in a supercapacitor is presented. The requirements for noise data recording are considered and correlated with working modes of supercapacitors. An example of results of low-frequency noise measurements in commercially available supercapacitors are presented. The ability of flicker noise measurements suggests that they can be used to assess quality of tested supercapacitors.

Keywords: supercapacitor, flicker noise, measurement set-up, reliability.

1. Introduction

Noise is known as an indicator for assessing quality and reliability of devices. It is widely used for semiconductor devices, sensors of various characters, electrochemical units, chemical reactions as corrosion, and other random phenomena [1–5]. Also, the use of noise methods can be studied for the assessment of capacitors' quality [6]. A detailed procedure is not obvious, as those devices are commonly used as elements for suppressing noise from circuits and therefore $1/f$ noise can be dominant at a very low frequency range only.

A supercapacitor is an electronic device that is capable of storing a relatively high amount of energy in comparison with its mass. On a Ragone plot, supercapacitors are placed between electrolytic capacitors and batteries [7]. Thanks to a very low series resistance, a supercapacitor can be charged and discharged very fast with a relatively high current. This, combined with a high number of charging-discharging cycles predestines it for applications that require management of peak powers and high dynamics. Typical applications of supercapacitors are energy storage systems with high current peaks, as in automotive applications for energy retrieval, energy harvesting and combined battery-supercapacitor systems.

Increasing popularity of supercapacitors and growing market of this devices require continuous development of methods for assessment of their quality and reliability. Nowadays, the most popular and commonly used methods for testing supercapacitors are: *cycling voltammetry* (CV), *galvano-static cycling with potential limitations* (GCPL), impedance spectroscopy and accelerated aging [8, 9]. All those methods are based on the observation of current or voltage during forced charging/discharging of a supercapacitor in various voltage and current conditions.

Quality of a supercapacitor is usually derived from its capacitance, equivalent series resistance, ESR, and impedance. Degradation of supercapacitor is indicated by the change of its capacity and ESR and is measured by known methods of estimation of those parameters.

Article history: received on Apr. 28, 2017; accepted on Jul. 31, 2017; available online on Dec. 10, 2017; DOI: 10.1515/mms-2017-0059.

2. Equivalent circuit of supercapacitor

One of types of supercapacitors is an *electric double layer capacitor* (EDLC). The EDLC comprises two porous carbon electrodes with an ion permeable separator and electrolyte solution between them. A typical EDLC structure is shown in Fig. 1.

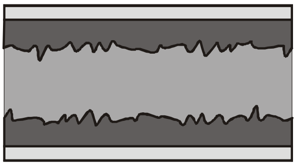

Fig. 1. An illustration of supercapacitor's structure.

When a supercapacitor is cyclically charged and discharged, four stages can be distinguished: 1) charging, when charges flow into the structure and a voltage increase is observed at the capacitor terminals; 2) a voltage drop, after the capacitor is charged and left with open terminals (the voltage at the terminals slowly decreases); 3) discharging, when charges flow out of the structure of capacitor, and a voltage drop is observed at the terminals and 4) the voltage restore, when the capacitor is discharged and left open-circuit (a voltage increase is observed between the terminals). A voltage curve when charging the supercapacitor with a constant current at disconnected terminals and discharging it with a constant current is shown in Fig. 2.

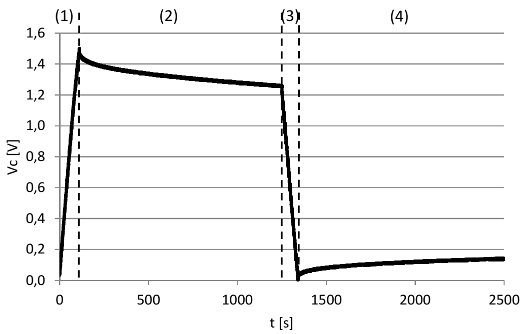

Fig. 2. A change of voltage between supercapacitor terminals during charging (1), when disconnected (2), (4) and during discharging (3).

An electrical equivalent circuit of supercapacitor that models its behaviour during the charging – discharging process is described in [10, 11]. The model comprises two branches, as shown in Fig. 3. The first branch with the equivalent series resistance ESR and capacitance C_H represents the Helmholtz layer capacity available for fast charging/discharging. The second one, with capacitance C_D and resistance R_D represents the mechanism of charges' redistribution by the diffusion mechanism [10, 12]. The electric capacitance of diffusion mechanism is represented by the capacitor C_D. The resistance R_D determines how fast is the diffusion mechanism. The resistance R_L represents the leakage current of the supercapacitor.

Metrol. Meas. Syst., Vol. 24 (2017), No. 4, pp. 645–652.

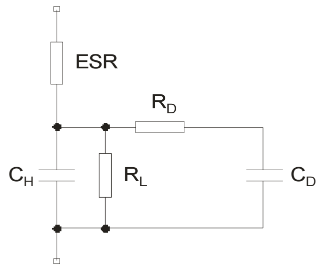

Fig. 3. A two-branch model of supercapacitor.

During stages 1 and 3, the charge is transported into and out of the structure, respectively. The charge is preserved in Helmholtz capacitance, as the value of R_D resistance is significantly higher than the value of ERS. In stage 2, when the charge stored in the structure is constant (the terminals are disconnected) we observe migration of the charge to pores that are less available and have not been yet occupied during the charging process. The time constant of this process is determined by diffusion resistance R_D and diffusion capacitance C_D (Fig. 3). Simplifying, the charge stored in Helmholtz capacitance C_H flows to diffusion capacitance C_D, which results in an overall voltage drop [10]. In this stage, also the leakage mechanism is responsible for the voltage drop. The leakage mechanism is dominant in this stage after relatively long time, while at the beginning it is the charge redistribution one that dominates [13].

In stage 4, when the supercapacitor is discharged and its terminals are open, an increase of voltage is observed between the terminals. It can be interpreted as an effect of a slow release of the charges stored deeply inside carbon pores. According to the electrical model (Fig. 3), after discharging Helmholtz capacitance C_H to zero volt and next opening the terminals, some amount of charge still remains in diffusion capacitance C_D because the resistance R_D is much higher than the ERS (the time constant $ESR{\cdot}C_H$ is smaller than the constant $R_D{\cdot}C_D$). Thus, the capacitance C_H will discharge faster than the capacitance C_D. Therefore, there will be a charge flow between C_H and C_D until the equilibrium state is reached [14].

When voltage is applied to the terminals of supercapacitor, ions migrate into vicinity of the electrode surface and form a Helmholtz plane. The electrode material is porous and ions migrate into pores, being forced by the electric field. Different size of pores and the random process of charging (penetration of pores at various speed) generates fluctuations in current flowing between the terminals when charged by a constant voltage supplied to the terminals. The fluctuations can be also observed during the discharging process when recording voltage fluctuations across the attached loading resistance.

The fluctuation phenomenon is induced by temperature (Johnson noise) but should exhibit some low frequency component (1/*f*-like noise) as well. That component should intensify when some areas of electrodes are on the verge of charging/discharging ability. We can assume that when some pores are blocked or almost blocked, the gathered charge can be removed (or stored) at a more slowly rate and low frequency fluctuations of that process should be observed. That phenomenon is observed in other electrochemical systems and applied to determine a corrosion rate [15].

Degradation of the supercapacitor as a result of operating conditions can be identified by an increase of ESR, a decrease of its electrical capacitance or by both mentioned changes. A decrease of capacitance is a result of blocking the pores by decomposed electrolyte and other chemical compounds. That degradation is irreversible. The pores can be also blocked by relatively large ions which exclude these pores from contributing to the supercapacitor terminal capacitance. These blocking processes are reversible and after some relaxation time can be at least partly restored .

Changes in the active area of carbon electrode (the number of active pores) should modify the intensity of fluctuation phenomenon. We can expect that the most intense 1/*f*-like noise is generated when the pores are on the verge of charging/discharging ability because such processes are rather very slow and will increase random components at a very low frequency range. When the pores are blocked completely, it means that these areas are excluded from any charging/discharging ability and noise generation as well. Thus, the 1/*f*-like noise should be potentially an interesting indicator of any process of pore blocking at its preliminary stage.

3. Low-frequency noise measurements in supercapacitor

A high value of capacitance C_H results in a very low frequency of low-pass filter formed by C_H, ESR and the loading resistance connected to the terminals of the tested supercapacitor. The electrical fluctuations are then filtered and only very low frequency components of noise generated inside the supercapacitor can be observed. This requires relatively long time of measurements because noise samples are recorded at very low rates. Moreover, estimation of power spectral density of noise samples requires averaging that lengthens the measurement process.

During the charging stage a stabilized current or voltage source is required to protect supercapacitor against overvoltage. These sources generate huge inherent noise or interference. It means that 1/*f*-like noise measurements during the charging stage could be overwhelmed by the inherent noise of the applied current or voltage source and therefore cannot be executed. Thus, we can assume that the low-frequency noise can be observed when the tested supercapacitor is fully charged (both capacitances C_H and C_D are completely charged) and some fluctuations are observed in the discharging current.

The supercapacitor can be discharged with a constant current or through a constant loading resistance. Discharging with a constant current shows the same limitations as charging with a constant current. An additional control unit is required which will introduce an additive noise source limiting identification of the 1/*f*-like noise component generated inside the discharged supercapacitor. That problem can be reduced when the supercapacitor is discharged through the joined constant loading resistance. A low-noise metallized resistor should be used for that aim. Moreover, when the supercapacitor is discharged through a resistance, the discharging time can be controlled by switching the loading resistor (*e.g.* between its low and high values). This method was applied for low-frequency noise measurements in the presented experimental studies.

A very low frequency noise component can be observed when the supercapacitor is discharged through a loading resistance securing a sufficiently low discharging current to record voltage fluctuations across the resistor for relatively long observation time. At the same time the discharging current should be huge enough to ensure intense voltage fluctuations across the loading resistor, up to the end of the recorded voltages.

A voltage across the loading resistor connected to the terminals of the charged capacitor is described by:

$$V(t) = V_0 \, e^{(-t/RC)}, \tag{1}$$

where: V_0 is an initial voltage between the terminals of the charged supercapacitor; R is a loading resistor and C is a capacitance. The discharging time could be estimated by:

$$t = -RC \ln (V/V_0), \tag{2}$$

where: V is an acceptable voltage in the final stage of noise recording. For example, a supercapacitor of 2,5 F capacitance charged to a voltage of 2,7 V and next discharged by

Metrol. Meas. Syst., Vol. 24 (2017), No. 4, pp. 645–652.

a loading resistor of 1 kΩ requires about 4 hours of discharging to reach a voltage between its terminals lower than 10 mV.

4. Measurement set-up

The measurement set-up for 1/*f*-like noise measurements in supercapacitor consists of (i) a current source with a voltage control, (ii) a switching unit with a set of keys (relays) to connect/disconnect supercapacitor to the elements of a bias circuit, (iii) a loading resistor and (iv) a data acquisition card (Fig. 4).

The controllable/programmable current source is used for charging/discharging of the examined supercapacitor before noise measurements. The current source is connected to the supercapacitor through the electronic keys in order to separate the supercapacitor and the current source during noise measurement. The keys are also used during measurements of charging/discharging currents and other parameters (*e.g.* a leakage current).

The data acquisition card provides dynamics and resolution of the recorded signals to measure AC (noise) and DC components of voltage ranging from a nominal voltage of the tested supercapacitor to nearly 0 V. The laboratory system secures 24-bit resolution and a voltage range of +/–10 V.

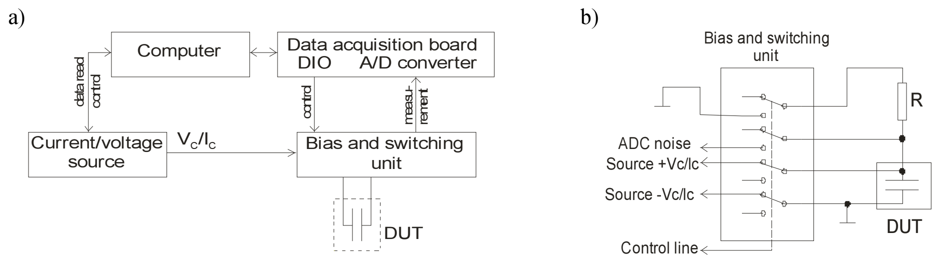

Fig. 4. The measurement setup: a block diagram (a); a switching and biasing unit (b).

Before noise measurements, the supercapacitor has to be charged to a given voltage. Moreover, its state should be stabilized. It is achieved either by leaving the supercapacitor with open terminals until its output voltage stabilizes (a voltage drop should be observed by a potentio-static cycle at a specific voltage until the current is sufficiently low, which indicates full charging of the tested supercapacitor – both C_H and C_D are fully charged). This operation is necessary to spread the charges within its structure. Next, the current/voltage source is disconnected and the loading resistor R and the data acquisition card are connected to the terminals of supercapacitor by the relay keys and voltage fluctuations across the loading resistor are recorded.

5. Experimental results and discussion

In the experiment, commercially available supercapacitors, DRL 2.7V 10F type, with a nominal capacitance 10 F and a nominal voltage 2.7 V, were used. A discharging curve of the tested supercapacitor discharged through the loading resistance 1 kΩ is shown in Fig. 5. An example of time record of voltage fluctuations and its histogram after removing the exponential trend are presented in Fig. 6.

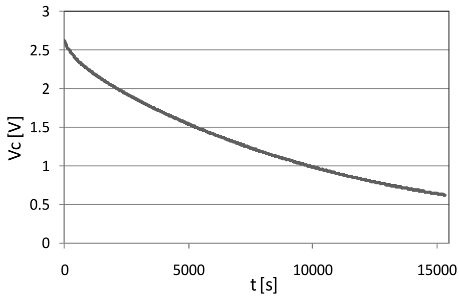

Fig. 5. A discharging curve of the tested supercapacitor, DRL 2.7V 10F type, through the loading resistance of 1 kΩ.

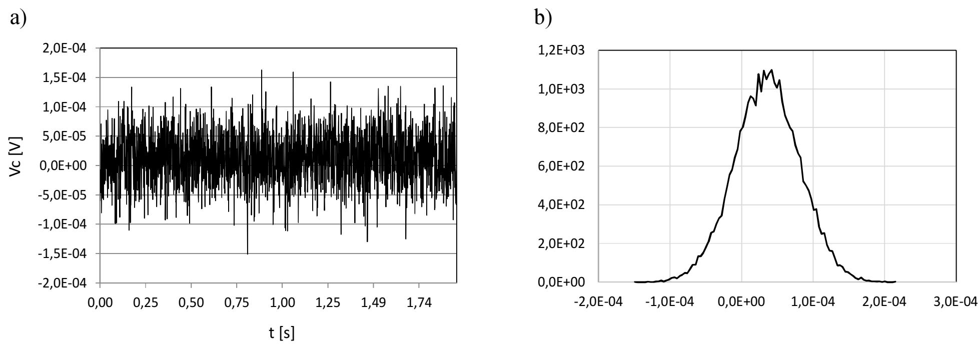

Fig. 6. An example of recorded time series of voltage fluctuations after removing the exponential trend (a) and its histogram (b).

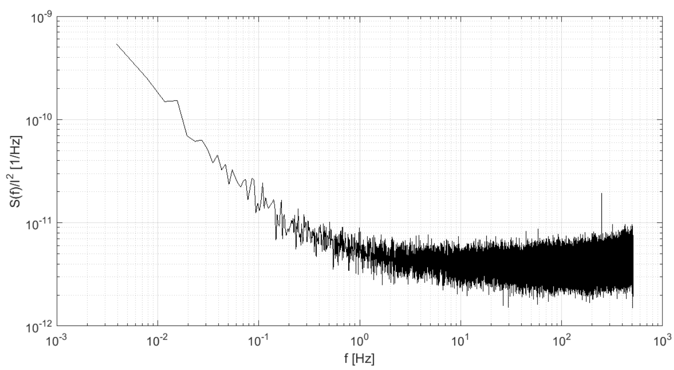

Fig. 7. Power spectral density of current fluctuations S(f) identified in the discharging current I of a DRL 2.7V 10F specimen when discharged through the loading resistance 1 kΩ. Power spectrum estimated in each time interval was normalized by the square of the discharging current.

The recorded samples were divided into sub-records and an FFT algorithm and the squaring operation was applied to estimate the power spectral density function S(f). The power spectra were normalized by the square of mean current I. The mean current value was calculated from the discharge current values in the time record the spectrum was calculated. Next, the spectra were averaged to reduce the estimation random error. An example of power spectrum density

Metrol. Meas. Syst., Vol. 24 (2017), No. 4, pp. 645–652.

is shown in Fig. 7. It required about 4 hours of noise recording and the 1/*f*-like noise dominates at low frequencies below 1 Hz. The presented results confirmed that the 1/*f*-like noise can be observed in supercapacitors and used to assess their quality. The recorded noise exhibited the 1/*f* noise. We suppose that some degradation processes in the supercapacitor structure change its slope as in the case of 1/*f*-like noise generated in other porous materials for gas sensing [16]. Such information should be valuable for quality assessment of the tested supercapacitors.

It should be underlined that the presented preliminary results depend on quality of not only the tested supercapacitors but also the materials used for their preparation (carbon electrodes and the type of electrolyte). Therefore, we cannot assure that the proposed measurements will give satisfactory results of 1/*f*-like noise measurements in other types of supercapacitors.

6. Summary

Low-frequency noise generated in supercapacitors requires carefully selected experiment conditions and relatively long time of data recording – up to a few hours – to estimate its power spectral density. The 1/*f*-like noise prevails at frequencies below 1 Hz only in the examined commercial supercapacitors. The proposed and prepared laboratory measurement set-up controls the measurement time by changing the value of loading resistor. Its value is a compromise between either obtaining a too low discharging current and observing a very tiny noise component or obtaining a too big discharging current during very fast discharging, reducing time for noise recording and making necessary the operation of averaging to reduce the random error of power spectral density estimation. Additional long-term study is required to determine how 1/*f*-like noise is related to quality of the tested supercapacitor.

The next important issue is whether the 1/*f*-like noise can be observed in an almost discharged supercapacitor when a small current flows between capacitances C_H and C_D. It would be very interesting because it should shed light on processes occurring inside the supercapacitor's structure which has not been examined with the above presented method .

Acknowledgment

This research was financed by the National Science Center, Poland, project No. DEC-2014/15/B/ST4/04957, "Charging/discharging mechanism at the electrode/electrolyte interface of supercapacitors". Decision of 11.05.2017.

References

[1] Smulko, J., Darowicki, K., Zieliński, A. (2002). Detection of random transients caused by pitting corrosion. *Electrochimica acta*, 47(8), 1297–1303.

[2] Kiwilszo, M., Smulko, J. (2009). Pitting corrosion characterization by electrochemical noise measurements on asymmetric electrodes. *Journal of Solid State Electrochemistry*, 13(11), 1681–1686.

[3] Smulko, J. (2006). Methods of electrochemical noise analysis for investigation of corrosion processes. *Fluctuation and Noise Letters*, 6(2), R1–R9.

[4] Smulko, J., Kish, B., Granqvist, G. (2007). Quality assessments of electrochromic devices: the possible use of 1/*f* current noise. *Ionics*, 13(3), 179–182.

[5] Vandamme, L.K.J. (1994). Noise as a Diagnostic Tool for Quality and Reliability of Electronic Devices. *IEEE Transactions On Electron Devices*, 41(11), 2116–2187.

[6] Konczakowska, A. (1998). 1/*f* noise of electrolytic capacitors as a reliability indicator. *Quality and Reliability Engineering International*, 14, 83–85.

[7] Kötz, R., Carlen, M. (2000). Principles and applications of electrochemical capacitors. *Electrochimica Acta*, 45(15–16), 2483–2498.

[8] Beguin, F., Frąckowiak, E. (2013). *Supercapacitors:Materials, Systems and Applications*. Wiley-VCH Verlag GmbH & Co. KGaA, Weinheim, Germany.

[9] Sedlakova, V., Sikula, J., Majzner, J., Sedlak, P., Kuparowitz, T., Buergler, B., Vasina, P. (2016). Supercapacitor Degradation Assesment by Power Cycling and Calendar Life Tests. *Metrol. Meas. Syst.*, 23(3), 345–358.

[10] Sedlakova, V., Sikula, J., Majzner, J., Sedlak, P., Kuparowitz, T., Buergler, B., Vasina, P. (2015). Supercapacitor equivalent electrical circuit model based on charges redistribution by diffusion. *Journal of Power Sources*, 286, 58–65.

[11] Szewczyk, A., Sikula, J., Sedlakova, V., Majzner, J., Sedlak, P., Kuparowitz, T. (2016). Voltage Dependence of Supercapacitor Capacitance. *Metrol. Meas. Syst.*, 23(3), 403–411.

[12] Yang, H., Zhang, Y. (2013). Analysis of Supercapacitor Energy Loss for Power Management in Environmentally Powered Wireless Sensor Nodes. *IEEE Transactions On Power Electronics*, 28(11), 5391–5403.

[13] Andreas, H.A. (2015). Self-Discharge in Electrochemical Capacitors: A Perspective Article. *Journal of The Electrochemical Society*, 162(5), A5047–A5053.

[14] Torregrossa, D., Bahramipanah, M., Namor, E., Cherkaoui, R., Paolone, M. (2014). Improvement of Dynamic Modeling of Supercapacitor by Residual Charge Effect Estimation. *IEEE Transactions On Industrial Electronics*, 61(3), 1345–1354.

[15] Smulko, J., Darowicki, K., Wysocki, P. (1998). Digital measurement system for electrochemical noise. *Polish Journal of Chemistry*, 72(7), 1237–1241.

[16] Lentka, Ł., Smulko, J.M., Ionescu, R., Granqvist, C.G., Kish, L.B. (2015). Determination of gas mixture components using fluctuation enhanced sensing and the LS-SVM regression algorithm. *Metrol. Meas. Syst.*, 22(3), 341–350.